Reversed dispersion slope photonic bandgap fibers for broadband dispersion control in femtosecond fiber lasers

Z. Várallyay[1*], K. Saitoh[2], J. Fekete[3], K. Kakihara[2], M. Koshiba[2], and R. Szipőcs[3,4]

[1] *Furukawa Electric Institute of Technology Ltd, Késmárk utca 24-28, H-1158 Budapest, Hungary*

[2] *Graduate School of Information Science and Technology, Hokkaido University, Sapporo 060-0814, Japan*

[3] *Research Institute for Solid State Physics and Optics, P.O. Box 49, H-1525 Budapest, Hungary*

[4] *R&D Ultrafast Lasers Ltd, P.O. Box 622, H-1539 Budapest, Hungary*

z.varallyay@feti.hu

Abstract: Higher-order-mode solid and hollow core photonic bandgap fibers exhibiting reversed or zero dispersion slope over tens or hundreds of nanometer bandwidths within the bandgap are presented. This attractive feature makes them well suited for broadband dispersion control in femtosecond pulse fiber lasers, amplifiers and optical parametric oscillators. The canonical form of the dispersion profile in photonic bandgap fibers is modified by a partial reflector layer/interface placed around the core forming a 2D cylindrical Gires-Tournois type interferometer. This small perturbation in the index profile induces a frequency dependent electric field distribution of the preferred propagating higher-order-mode resulting in a zero or reversed dispersion slope.

OCIS codes: (060.2280) Fiber design and fabrication; (060.5295) Photonic crystal fibers.

References and links

1. M. Wandel and P. Kristensen, "Fiber designs for high figure of merit and high slope dispersion compensating fibers," J. Opt. Fiber. Commun. Rep. **3,** 25-60 (2005).
2. L. Grüner-Nielsen, M. Wandel, P. Kristensen, C. Jørgensen, L. V. Jørgensen, B. Edvold, B. Pálsdóttir, and D. Jakobsen, "Dispersion-Compensating Fibers," J. Lightwave Technol., **23,** 3566-3579 (2005).
3. S. Ramachandran, S. Ghalmi, J. W. Nicholson, M. F. Yan, P. Wisk, E. Monberg, and F. V. Dimarcello, "Anomalous dispersion in a solid, silica-based fiber," Opt. Lett. **31,** 2532-2534 (2006).
4. J. W. Nicholson, S. Ramachandran, and S. Ghalmi, "A passively-modelocked, Yb-doped, figure-eight, fiber laser utilizing anomalous-dispersion higher-order-mode fiber," Opt. Express **15,** 6623-6628 (2007).
5. P. St. J. Russell, "Photonic-Crystal Fibers," J. Lightwave Technol. **24,** 4729-4749 (2006).
6. J. Jasapara, T. H. Her, R. Bise, R. Windeler, and D. J. DiGiovanni, "Group-velocity dispersion measurements in a photonic bandgap fiber," J. Opt. Soc. Am. B **20,** 1611-1615 (2003).
7. C. K. Nielsen, K. G. Jespersen, and S. R. Keiding, "A 158 fs 5.3 nJ fiber-laser system at 1 μm using photonic bandgap fibers for dispersion control and pulse compression," Opt. Express **14,** 6063-6068 (2006).
8. A. Ruehl, O. Prochnow, M. Engelbrecht, D. Wandt, and D. Kracht, "Similariton fiber laser with a hollow-core photonic bandgap fiber for dispersion control," Opt. Lett. **32,** 1084-1086 (2007).
9. C. de Matos, J. Taylor, T. Hansen, K. Hansen, and J. Broeng, "All-fiber chirped pulse amplification using highly-dispersive air-core photonic bandgap fiber," Opt. Express **11,** 2832-2837 (2003).
10. J. C. Knight, "Photonic crystal fibers," Nature **424,** 847-851 (2003).
11. K. Saitoh and M. Koshiba, "Leakage loss and group velocity dispersion in air-core photonic bandgap fibers," Opt. Express **11,** 3100-3109 (2003).

#96268 - $15.00 USD Received 20 May 2008; revised 24 Jul 2008; accepted 12 Sep 2008; published 18 Sep 2008

12. B. Rózsa, G. Katona, E. S. Vizi, Z. Várallyay, A. Sághy, L. Valenta, P. Maák, J. Fekete, Á. Bányász, and R. Szipőcs, "Random access three-dimensional two-photon microscopy," Appl. Opt. **46,** 1860-1865 (2007).
13. D. G. Ouzonov, F. R. Ahmad, D. Müller, N. Venkataraman, M. T. Gallagher, M. G. Thomas, J. Silcox, K. W. Koch, and A. L. Gaeta, "Generation of Megawatt optical solitons in hollow-core photonic band-gap fibers," Science **301,** 1702-1704 (2003).
14. D. G. Ouzounov, Ch. J. Hensley, A. L. Gaeta, N. Venkateraman, M. T. Gallagher, and K. W. Koch, " Soliton pulse compression in photonic band-gap fibers" Opt. Express **13,** 6153-6159 (2005).
15. Q. Fang, Z. Wang, L. Jin, J. Liu, Y. Yue, Y. Liu, G. Kai, S. Yuan, and X. Dong, "Dispersion design of all-solid photonic bandgap fiber," J. Opt. Soc. Am. B **24,** 2899-2905 (2007).
16. G. Vienne, Y. Xu, C. Jakobsen, H. J. Deyerl, J. Jensen, T. Sorensen, T. Hansen, Y. Huang, M. Terrel, R. Lee, N. Mortensen, J. Broeng, H. Simonsen, A. Bjarklev, and A. Yariv, "Ultra-large bandwidth hollow-core guiding in all-silica Bragg fibers with nano-supports," Opt. Express **12,** 3500-3508 (2004).
17. J. Fekete, Z. Várallyay and R. Szipőcs, "Design of leaking mode free hollow core photonic bandgap fibers," **JWA4,** OFC/NFOEC Conference, San Diego, CA, 2008.
18. P. Yeh, A. Yariv, and E. Marom, "Theory of Bragg fiber" J. Opt. Soc. Am. **68,** 1196-1201 (1978).
19. I. T. Sorokina, E. Sorokin, E. Wintner, A. Cassanho, H. P. Jenssen, R. Szipőcs, "Prismless passively mode-locked femtosecond Cr:LiSGaF laser," Opt. Lett. **21,** 1165-1167 (1996).
20. R. Szipőcs, A. Kőházi-Kis, S. Lakó, P. Apai, A. P. Kovács, G. DeBell, L. Mott, A. W. Louderback, A. V. Tikhonravov, and M. K. Trubetskov, "Negative dispersion mirrors for dispersion control in femtosecond lasers: chirped dielectric mirrors and multi-cavity Gires-Tournois interferometers," Appl. Phys. B **70,** S51-S57 (2000).
21. H. A. Macleod, "Thin-film optical filters," 3rd edition (Taylor & Francis Group, Oxon, GB, 2001).
22. S. Février, R. Jamier, J.-M. Blondy, S. L. Semjonov, M. E. Likhachev, M. M. Bubnov, E. M. Dianov, V. F. Khopin, M. Y. Salganskii, and A. N. Guryanov, "Low-loss single mode large mode area all-silica photonic bandgap fiber," Opt. Express **14,** 562-569 (2006).
23. http://www.cvilaser.com/Common/PDFs/dispersion_equations.pdf
24. Z. Várallyay, J. Fekete, and R. Szipőcs, "Higher-order mode photonic bandgap fibers with reversed dispersion slope," **JWA8,** OFC/NFOEC Conference, San Diego, CA, 2008.
25. K. S. Lee, and T. Erdogan, "Fiber mode conversion with tilted gratings in an optical fiber," J. Opt. Soc. Am. A **18**, 1176-1185 (2001).
26. A. Ferrando, E. Silvestre, J. J. Miret, P. Andrés, and M. V. Andrés, "Full-vector analysis of realistic photonic crystal fiber," Opt. Lett. **24,** 276-278 (1999).
27. K. Saitoh, M. Koshiba, T. Hasegawa, and E. Sasaoka, "Chromatic dispersion control in photonic crystal fibers: application to ultra-flattened dispersion," Opt. Express **11,** 843-852 (2003).
28. G. K. L. Wong, S. G. Murdoch, R. Leonhardt, J. D. Harvey, and V. Marie, "High-conversion-efficiency widely-tunable all-fiber optical parametric oscillator," Opt. Express **15,** 2947-2952 (2007).
29. R. Amezcua-Correa, N. G. Broderick, M. N. Petrovich, F. Poletti, and D. J. Richardson, "Optimizing the usable bandwidth and loss through core design in realistic hollow-core photonic bandgap fibers," Opt. Express **14,** 7974-7985 (2006).
30. M. Foroni, D. Passaro, F. Poli, A. Cucinotta, S. Selleri, J. Lægsgaard, A. Bjarklev, and V. Marie, "Tailoring of the transmission window in realistic hollow-core Bragg bers," **JWA7,** OFC/NFOEC Conference, San Diego, CA, 2008.
31. T. Murao, K. Saitoh, and M. Koshiba, "Structural optimization of ultimate low loss air-guiding photonic bandgap fibers," **JWA5,** OFC/NFOEC Conference, San Diego, CA, 2008.

1. Introduction

The demand for all-fiber devices is continuously growing due to their environmental stability, compactness, cost efficiency and maintenance-free operation. Ultrashort pulsed fiber lasers and amplifiers should also comprise more and more fiber-integrated and spliced optical elements. Ultrashort pulse ($<$ 100 fs) generation from an oscillator or an amplifier, however, requires dispersion control even in higher orders. Dispersion compensating fibers [1, 2] or higher-order-mode (HOM) fibers [3] can meet this requirement. Sub-100 fs fiber laser operation at around 1 micron utilizing a HOM fiber for intra- and extracavity dispersion control has already been demonstrated [4]. Although HOM fibers are nearly perfect solutions for dispersion control in low-power oscillators, the nonlinear contribution may harm the temporal and spectral properties of the generated femtosecond pulses above certain intensities because of their solid cores (SC). Higher energy pulses generated by femtosecond pulse fiber amplifiers are preferred to be compressed by hollow core (HC) fibers [5], which exhibit low nonlinearity, since most of the

#96268 - $15.00 USD Received 20 May 2008; revised 24 Jul 2008; accepted 12 Sep 2008; published 18 Sep 2008

optical power is guided in the air core. It is also an important fact that air-silica and in some cases solid core photonic bandgap (PBG) fibers exhibit anomalous dispersion over most of their bandgaps [5, 6]. PBG fibers with properly tailored dispersion profile could be well suited for intracavity dispersion compensation in ultrashort pulse fiber oscillators [7, 8] and for coupling free pulse compression in fiber amplifiers [9].

The dispersion profile of state of the art photonic bandgap fibers has the "canonical form" for bandgap guidance, which is basically a third-order function monotonically increasing from short to longer wavelengths. Additionally, the third- and higher-order dispersion terms are considerable at around the center of the bandgap, where the second-order dispersion (D) is relatively low [6, 10, 11]. Such a dispersion profile does not provide appropriate conditions for ultrashort pulse generation or compression, since the residual third- and higher-order dispersion terms result in strongly distorted pulses with satellite pulses after compression. For most applications, such as time resolved spectroscopy, nonlinear optics including nonlinear microscopy, etc., however, nearly transform limited, high quality optical pulses are preferred. In time resolved spectroscopy, for instance, the pump and probe pulses must have a definite "start" in order to define the time scale of the investigated chemical, biological or physical processes. Nonlinear optical applications such as nonlinear frequency conversion techniques or nonlinear microscopy [12] call for high peak intensity pulses at minimum average power in order to increase the signal to noise ratio in optical imaging systems or minimize the heating (and aging) of the sample. The experimental results during the first demonstration of soliton compression in HC PBG fibers [13] showed also that, due to the frequency dependent dispersion profile of the hollow core PBG fiber, the compressed pulse exhibited some considerable temporal and spectral asymmetry. In a subsequent publication the same authors showed that the large TOD of the Xe filled HC fibers they used in the experiments degraded the optimal compression ratio to a factor of 2.4. They pointed out that in order to achieve higher compression ratios for femtosecond pulses, efforts need to be made to reduce the TOD in these fibers [14].

Experimental observations that (i) waveguide contribution to the dispersion of PBG fibers can be significant and (ii) Fabry-Perot like resonances (leaking or surface modes) appearing within the bandgap cause an inflection on the dispersion profile [6] indicated the possibility of dispersion modification in PBG fibers. Some numerical simulations also showed that structural modifications such as defect rods in a PCF cladding may vary the dispersion function [15] for the LP_{01} mode. Such a modification, however, does not result in a reversed or zero dispersion slope of the fiber.

A close analogy between 1D (plane) PBG structures such as dielectric mirrors at grazing incidence of light and 2D (cylindrical) PBG fibers has been established [16, 17]. Using this analogy, as a first step, we calculate the dispersion and loss profiles for solid core (SC) [18] and hollow core (HC) Bragg PBG fibers [16, 17] in this paper. For both structures, we propose some structural modifications on the PBG waveguide cross-section, which results in a zero or reversed dispersion slope for certain propagating modes (LP_{02}) within the bandgap. The 1D simulation results presented in Section 2 are followed by corresponding 2D simulations in Section 3, which are based on the vector finite element (FE) modeling and the Helmholtz eigenvalue equation with a surrounding perfectly matched layer (PML). Later on, we present our 2D simulation results for all-silica, air core PBG fibers of honey-comb structure using the same numerical method. We show that a similar slight structural modification, i.e., a certain displacement of the first thin silica ring around the core can also result in a reversed dispersion slope of the modified honey-comb structure. The presented moderate loss, high damage threshold, leaking mode-free dispersive fiber optic devices could be well suited for dispersion control in ultrafast fiber laser applications including all-fiber femtosecond fiber lasers, amplifiers, fiber optic parametric oscillators as well as fiber delivery and imaging systems.

#96268 - $15.00 USD Received 20 May 2008; revised 24 Jul 2008; accepted 12 Sep 2008; published 18 Sep 2008

2. 1D modeling

In this Section, we investigate the question how the "canonical form" of the dispersion profile of 1D and 2D PBG structures can be modified by some structural modifications. For these studies, we use the 1D model previously developed for design of dispersive dielectric mirror structures utilized in fs pulse solid state laser systems [19, 20]: the (reflection) loss, the group delay and dispersion of the Bragg structures are calculated by the transfer matrix method [21].

In order to obtain a photonic bandgap centered at a certain wavelength λ_0, optical thicknesses of the different (1D plane or 2D cylindrical) layers should be calculated using the following expression:

$$OT_m = n_m d_m \cos\alpha_m = \lambda_0/4 \quad \text{where} \quad m = L \text{ or } H \tag{1}$$

where L and H indicate that the parameter belongs to the low or high index layer, respectively. In (1), n is the refractive index, d is the physical thickness of the corresponding layer, α is the angle of refraction and λ_0 is the preferred center of the bandgap. This requirement is often referred to as the quarter wave (QW) condition for the optical thicknesses of the layers. Using the Snell law and some trigonometry, the physical thicknesses of the layers can be expressed with the angle of incidence of light (at the core/cladding interface)

$$d_m = \frac{\lambda_0}{4\sqrt{n_m^2 - n_c^2 \sin^2\Theta}} \tag{2}$$

where Θ is the angle of incidence and n_c is the refractive index of the core or the refractive index of the environment in the case of thin films (TF). Eq. (2) is applied for calculating the physical thicknesses of layers in Bragg structures for which the angle of incidence (Θ) reaching a 2D Bragg structure is obtained from the FE calculations: the eigenvalue and the corresponding effective index value for a certain propagating mode determines the angle of incidence at the core/cladding interface:

$$\Theta(\lambda) = \arcsin\left(\frac{n_{\text{eff}}(\lambda)}{n_c(\lambda)}\right) \tag{3}$$

where n_{eff} is the effective index obtained from the solution of the Helmholtz eigenvalue equation. For the corresponding 1D model, we use this $\Theta(\lambda)$ function as a (wavelength dependent) angle of incidence.

During the design procedure, we found that the design equations presented above work well for hollow core PBG structures, however, in case of solid core PBG fibers they can not be used due to the non-zero or π phase shifts at the layer interfaces. In the case of solid core PBG fiber structures, we used numerical optimization to determine the optimum high and low index layer thicknesses providing the highest reflection (lowest confinement loss) and the broadest photonic bandgap [20].

In the following numerical examples, we aim for designing PBG fibers exhibiting the desired dispersion profile and photonic bandgaps at around the Ytterbium wavelength. Accordingly, the corresponding 1D simulations are performed for a layered dielectric media exhibiting a photonic bandgap at around 1.03 micron, in which we demonstrate the possibility of tailoring the dispersion profile (i.e., adjusting the dispersion slope (S)) of SC and HC type fibers by applying slightly coupled cavities located at the top of the Bragg mirror structure.

The first 1D model corresponds to a SC Bragg fiber comprising five periods of alternate low and high index layers of "quarterwave" optical thicknesses. The light reaches the Bragg structure from a fused silica (FS) environment (Fig. 1(a)). The refractive index of the low index layer is chosen to be equal to that of fused silica glass, while the refractive index of the high index glass is increased by the wavelength independent value of $\Delta n = 0.05$, which can be

#96268 - $15.00 USD Received 20 May 2008; revised 24 Jul 2008; accepted 12 Sep 2008; published 18 Sep 2008

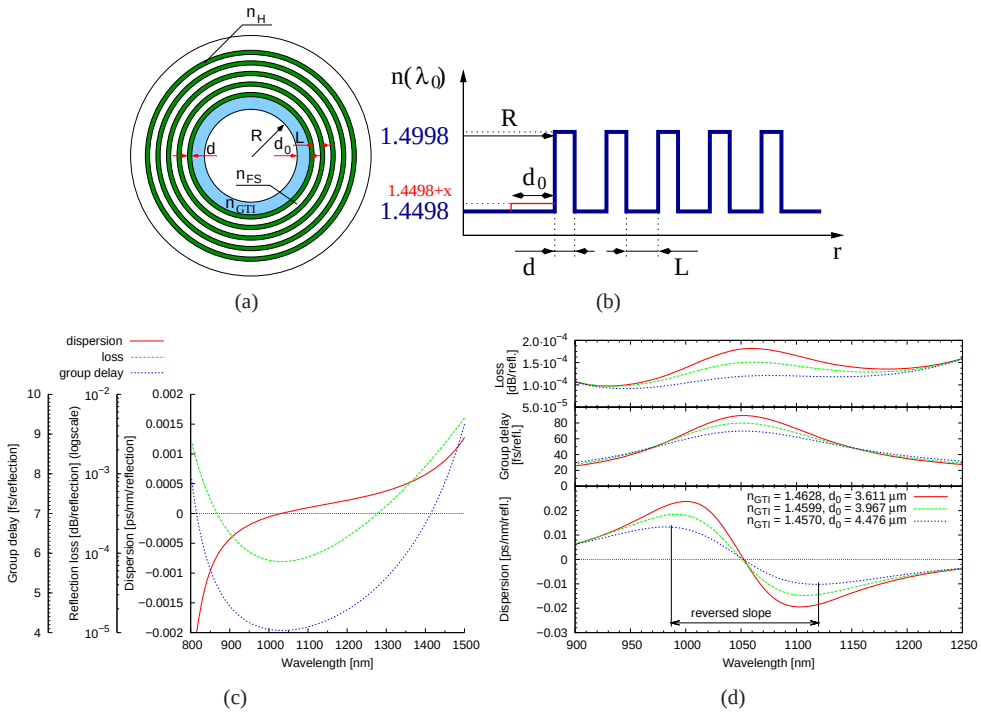

Fig. 1. (a) SC Bragg PBG fiber used for FEM calculations, (b) 1D equivalent of a SC Bragg PBG fiber, (c) dispersion, loss and group delay of the 1D structure comprising 5 periods of low and high index layers with 2.543 μm and 0.651 μm thicknesses, respectively, (d) and demonstration of the reversed dispersion slope applying different GTI cavities on the top of the Bragg structure.

obtained by Ge doping [22]. For the sake of simplicity, the solid core is also made of FS in our model (Fig. 1(a) and (b)). The wavelength dependent refractive index of the FS core and the FS layers is calculated using the Sellmeier equations (see, for instance, at Ref. [23]). In our previous studies [24], we included FS and SF10 glass layers, which resulted in a higher index difference and hence a higher bandwidth and lower confinement loss. From a technological point of view (fiber drawing process), however, certainly it was not the perfect material pair to choose. In this paper, we present SC Bragg fiber designs and corresponding 1D and 2D simulation results that could be easily manufactured making a preform by Modified Chemical Vapor Deposition (MCVD) process [22].

Using the computer optimization process mentioned above for a propagation angle of $\sim 86^\circ$ at the core-cladding interface, we can obtain a 1D structure composed of low index FS and high index Ge doped FS layers exhibiting a bandgap at around one micron. In order to find the optimum layer thicknesses, the merit function comprises two requirements during the optimization process: one for the highest reflectivity and one for zero group delay dispersion (GDD) at our reference wavelength of 1030 nm. The periodic Bragg structure has low and high index layers of physical thicknesses of 2.543 μm and 0.651 μm, respectively. The computed (reflection) loss, the group delay and dispersion of the solid core Bragg structure are shown in Fig. 1(c). We must note here that in these 1D calculations the (reflection) loss is given in dB/reflection units. However, in order to compare these results to the 2D results described in Section 3, we can say that a relationship between the fiber confinement loss and the reflection

#96268 - $15.00 USD Received 20 May 2008; revised 24 Jul 2008; accepted 12 Sep 2008; published 18 Sep 2008

loss can be derived. The "number of reflections" at the core/cladding interface along a one meter long fiber can be calculated using the "angle of incidence" and the core diameter, which calculation is based on a geometrical optics approach. Using some trigonometry, the distance between two reflections can be determined. The inverse of the distance between two reflections gives the number of reflections along 1 m of propagation length. Multiplying the loss given in dB/reflection units by the number of reflections will give approximately the confinement loss in dB/m units.

In the following, we modify the dispersion profile of the 1D thin film (TF) structure by introduction of a partial reflector layer/interface at the top of the core forming a slightly coupled cavity. In ultrafast thin film optics, this is often referred to as a (single-cavity) thin film Gires-Tournois interferometer (GTI) type dielectric mirror structure, and have been successfully applied for second- and third-order dispersion control in sub-100 fs pulse laser systems [19]. In contrast to thin-film devices used typically at normal incidence of light, we must note that the application of GTI type cavities in 2D Bragg fibers is preferred around the core region due to the relatively high Fresnel reflection at the high and low index layer interfaces.

Introducing a new layer around the core with a slightly increased refractive index of 1.4628 ($\Delta n = 0.013$) relative to FS core and choosing the thickness of this layer 1.42 times wider than that of the low index QW thickness, we may obtain a reversed dispersion slope around 1.05 μm over a wavelength range of 104 nm (see Fig. 1(d)). Decreasing the refractive index of the partial reflector layer and increasing d_0 (see Fig. 1(b)), the wavelength range where reversed dispersion slope can be achieved is broadened. The parameters of some calculated structures and their results are summarized in Table 1.

Table 1. Summary of 1D simulation data corresponding to GTI type SC Bragg fibers of different designs exhibiting reversed dispersion slope.

Index of refraction of GTI (n_{GTI})	Width of GTI layer (d_0)	Bandwidth of reversed slope
1.4628	3.611 μm	104 nm
1.4614	3.764 μm	110 nm
1.4599	3.967 μm	118 nm
1.4585	4.1832 μm	127 nm
1.4570	4.4757 μm	139 nm

We performed similar calculations for the 1D equivalent of a HC Bragg fiber, which comprise silica and air layers as a Bragg mirror (see Fig. 2(a)). The effect of support bridges between silica layers were considered by increasing the effective index of low index layers by a few percent [17]. Using Eq. (2), we calculated physical thicknesses of the FS and air "layers" of the Bragg structure, and obtained values of 0.25 μm and 5 μm, respectively, when we assume that the fundamental mode propagates at an angle of incidence of 87° around 1.05 μm. The results we obtained for 1D equivalent of the QW Bragg fiber design (Fig. 2(b)) is summarized in Fig. 2(c), where the computed dispersion profile, reflection loss and group delay are shown.

In order to reverse the dispersion slope, a very thin partial reflector layer providing a low Fresnel reflection for the 2D GTI type cavity has to be introduced next to the core with some spacer layer between. One possible 2D realization is shown in Fig. 2(a). We note that a properly "detuned" first period comprising the inner high and low index layers may also result in a structure that causes a broadband resonance in the frequency dependent standing wave field distribution in the structure.

For a partial reflector having a thickness of 10% compared to the original high index QW stack design the spacer L_0 (Fig. 2(a)) has to be set 0.34 times smaller than the original low index layer. This structure results in a reversed dispersion slope from 915 nm to 1230 nm altogether

#96268 - $15.00 USD Received 20 May 2008; revised 24 Jul 2008; accepted 12 Sep 2008; published 18 Sep 2008

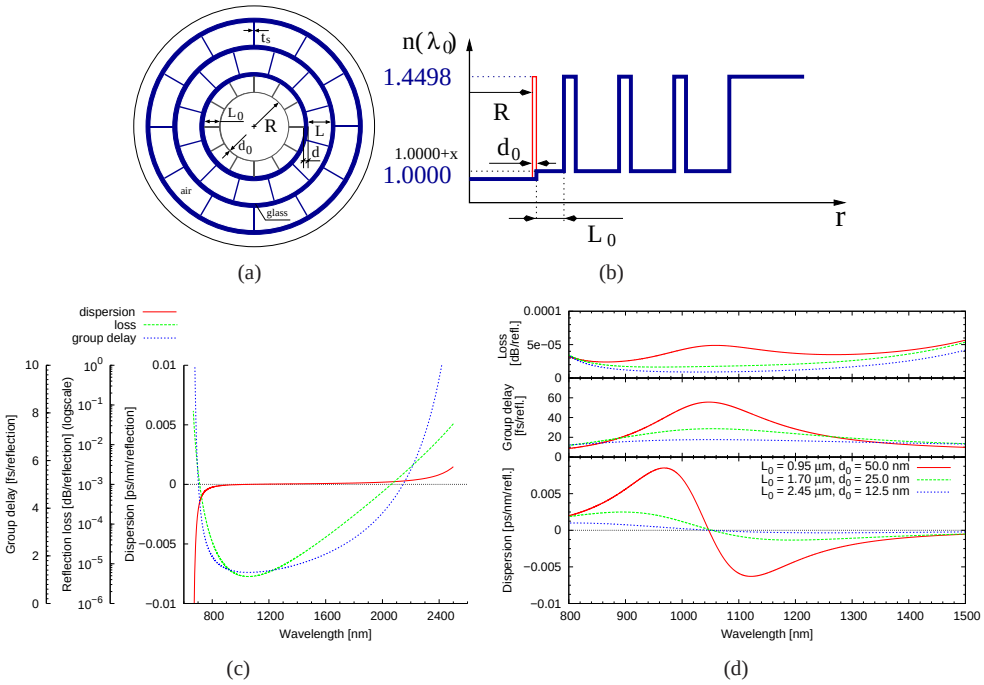

Fig. 2. (a) Scheme of the all-silica Bragg fiber cross section used for FEM simulations, (b) 1D equivalent of all-silica Bragg structure with the additional GTI layer next to the core (red line), (c) computed dispersion, loss and group delay of the 1D equivalent without GTI layer, (d) computed dispersion loss and phase delay of the 1D equivalent with different GTI layer designs.

315 nm at around 1.05 μm (Fig. 2(d)). Some additional calculation results are listed in Table 2 and plotted in Fig. 2(d).

Finally, we note that reversed dispersion slope can also be achieved in a limited wavelength range by simply reducing the thickness of the first low index layer around the core without changing the thickness of the core wall. Related calculations are presented in Section 3.3 related to HC fiber of honey-comb cladding structure.

Table 2. Summary of 1D simulation data corresponding to GTI type HC Bragg fibers of different designs exhibiting reversed dispersion slope.

High index layer of GTI (d_0)	Low index layer of GTI (L_0)	Bandwidth of reversed slope
12.5 nm	2.45 μm	490 nm
25 nm	1.70 μm	315 nm
50 nm	0.95 μm	155 nm

3. 2D modeling

Based on the results presented in Section 2, we expect that by applying partial reflector layers forming 2D Gires-Tournois interferometer type cavities around the core [19, 20], one can reverse the dispersion slope of PBG fibers. This physical effect can result in anomalous or nearly zero dispersion with a flat cumulative dispersion profile in any all-fiber device. Partial reflector

#96268 - $15.00 USD Received 20 May 2008; revised 24 Jul 2008; accepted 12 Sep 2008; published 18 Sep 2008

layers, however, perform better for higher-order propagating modes in 2D PBG structures. In order to couple the light from a single mode fiber to the preferred higher-order-mode of the presented PBG structures, one has to apply high efficiency mode converters [25]. Such devices were previously successfully applied in passively mode-locked Yb fiber laser utilizing anomalous dispersion higher-order-mode fiber [4]. When the preferred higher-order-mode is excited in 2D PBG structures of the presented 2D GTI design, we obtain such a wavelength dependent transversal electromagnetic field distribution around the core, which is capable to reverse the dispersion slope over a certain wavelength regime within the bandgap.

2D analysis of the fibers can be done by the Helmholtz eigenvalue equation using FE analysis [26, 27]. The obtained eigenvalue for the appropriate mode can be used to determine the dispersion and loss properties of the investigated waveguide. The real part of the obtained effective index has a relation to the dispersion as follows

$$D(\lambda) = \frac{\lambda}{c}\frac{d^2 \Re n_{\text{eff}}}{d\lambda^2} \tag{4}$$

where c is the speed of the light in vacuum, n_{eff} is the effective refractive index, λ is the free space wavelength and $\Re$ stands for the real part. If a PML is applied around the geometry, the eigenvalue is complex, and its imaginary part yields the confinement loss of the calculated mode

$$\alpha_{cf}(\lambda) = \frac{2\pi}{\lambda}\Im n_{\text{eff}} \tag{5}$$

where $\Im$ stands for the imaginary part. In order to obtain the loss in dB/m, Eq. (5) must be multiplied by $10/\ln(10)$.

In what follows we analyze the dispersion and loss properties of SC and HC Bragg fibers along with PBG fibers in a general context. We present novel structural modifications relating to the 1D PBG structures presented above which yield the possibility of dispersion management in PBG fibers.

3.1. SC Bragg fiber

The SC Bragg fiber design comprises five periods of alternating low and high index materials in the cladding region (see Fig. 1(a)), where the low index cylindrical layer is made of FS, same as the core, while the high index layers are made of Ge doped FS ($\Delta n = 0.05$). The refractive indices and the layer thicknesses for high and low index layers used in the FE calculations are the similar to that we used for the corresponding 1D simulations; $d = 0.651$ μm and $L = 2.543$ μm, respectively. The additional cylindrical GTI layer in our model has a physical thickness of $d_0 = 3.992$ μm and a refractive index of 1.4643 at around 1.05 μm.

The LP_{02} mode as well as the fundamental LP_{01} mode has a suitable transversal distribution to show the required 2D GTI effect. In Ref. [24], we demonstrated this effect for the LP_{02} mode in a Bragg fiber composed of FS and SF10 glass cylindrical layers. Here, in Fig. 3(a) we show the computed dispersions and confinement losses corresponding to the LP_{01} and the LP_{02} modes in the Bragg fiber described above. In case of the LP_{01} mode, the structure provides a 150 nm wide negative (reversed) dispersion slope (from 800 nm to 950 nm) and a normal dispersion. In case of the LP_{02} mode, the structure exhibits a 80 nm wide reversed dispersion slope regime from 690 nm to 775 nm. In contrast to the LP_{01} mode, the dispersion is positive (anomalous) in the wavelength range of 690 to 730 nm. In Fig. 3(b) and (c), we respectively show the computed mode field distributions for the LP_{01} and the LP_{02} modes at different wavelengths. In case of the LP_{01} mode, we find that at the resonance wavelength of 800 nm, the electric field is localized in the cylindrical GTI layer, while at around 1 micron, far enough from the resonance wavelength, we obtain a mode field distribution basically of the fundamental mode.

#96268 - $15.00 USD Received 20 May 2008; revised 24 Jul 2008; accepted 12 Sep 2008; published 18 Sep 2008

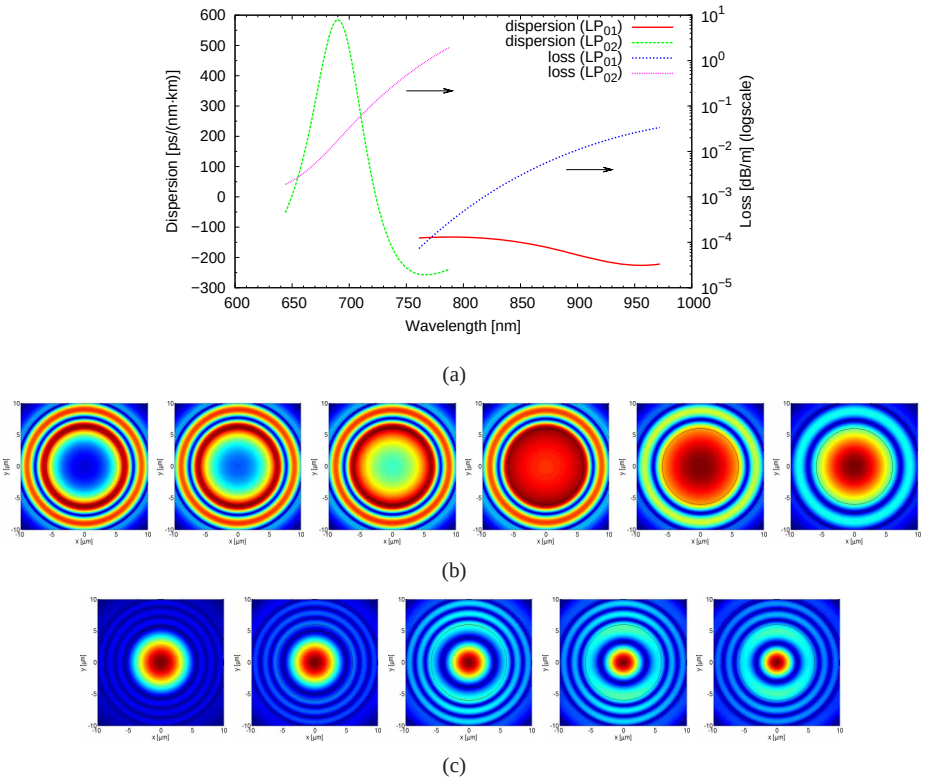

Fig. 3. Results of finite element modeling: (a) dispersion and loss properties of a solid core Bragg PBG fiber with a resonant Gires-Tournois layer around the core, (b) corresponding mode field distributions at wavelengths of 800, 850, 900, 950, 1000 and 1050 nm (from left to right) which modes have LP_{01} field distribution in the core for longer wavelengths, (c) LP_{02} mode distributions at wavelengths of 640, 680, 720, 760 and 800 nm.

Between these two wavelengths, the mode field distribution continuously varies from one to another. In case of the LP_{02} mode, the behavior is similar, but this mode could be excited more easily by application of a mode converter [25]. By rescaling the layer thicknesses, both center of the bandgap and the reversed dispersion slope regime could be centered at any wavelength at around one micron. Further expansion of the negative dispersion slope regime resulting in a nearly constant net zero dispersion over a wide wavelength range could be advantageous in construction of broadly tunable fiber optical parametric oscillators [28].

3.2. HC Bragg fiber

We used three periods of high (glass) and low (air) index layers in our HC Bragg fiber model (Fig. 2(a)). We neglected the effect of silica struts between the glass layers in a first approximation, though these small structural parts modify the effective index of the low index layers by a few percent which requires the modification of the fiber cross-section parameters [17]. Silica struts also introduce some mode anti-crossing events due to the lowering of symmetry from full cylindrical (C_∞). Due to the significance of small details in PBG structures which can be crucial in the design of reliable PBG waveguides, a more accurate model is presented afterwords. We must note however, that the purpose of this paper is to demonstrate the dispersive effect of a

#96268 - $15.00 USD Received 20 May 2008; revised 24 Jul 2008; accepted 12 Sep 2008; published 18 Sep 2008

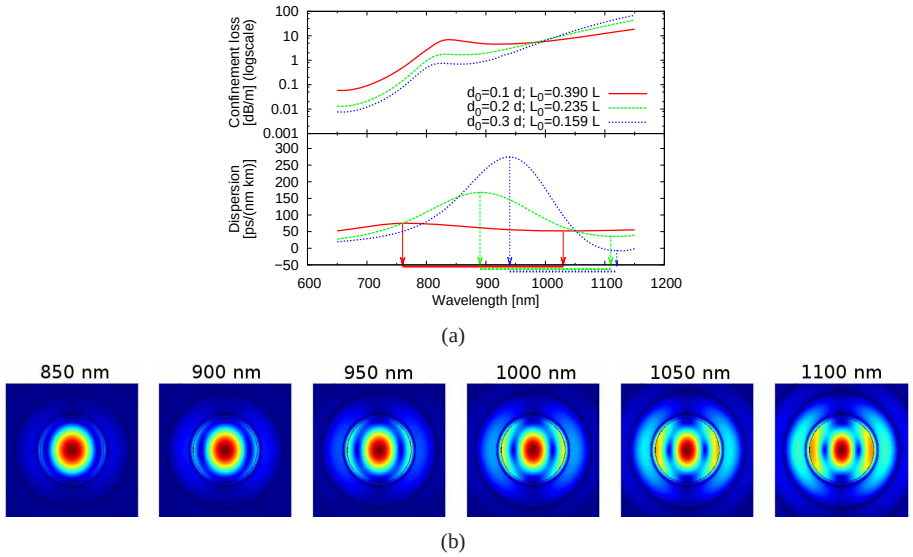

Fig. 4. (a) Dispersion and confinement loss of LP_{02} mode propagating in HC Bragg fiber corresponding to three different 2D GTI structures. High and low index thicknesses are $d = 0.25$ μm and $L = 3.92$ μm in the QW Bragg mirror structure. Physical thicknesses of the high index partial reflector layers (d_0) and the low index air spacer layers (L_0) forming the 2D GTI structure are given as functions of the high and low index QW layer thicknesses. (b) LP_{02} mode field distribution in a HC Bragg fiber having a 2D GTI structure with design parameters $d_0 = 0.3d$ and $L_0 = 0.3L$. (blue curve in Fig. 4(a)).

properly designed GTI layer applied in a PBG fiber, but solving the leaking mode problem is an additional issue on which many efforts are being made recently [11, 29]. In the case of HC all-silica Bragg fibers, the leaking-mode problem is still unsolved but some improvements such as decreasing the number of mode anti-crossing events and increasing the size of the transmission window by choosing alternating sizes for the low index layers have already been published [30].

Based on Eqs. (2) and (3), we obtained a critical angle of incidence at 86.16 degrees using the eigenvalues from FE analysis resulting in the thicknesses for the low and high index layers being 3.92 and 0.25 μm, respectively.

The GTI layer can be formed by readjusting the first high and low index layers around the core. The thin glass layer plays the role of the partial reflector, and behind the resized low index layer (cavity), the first high index layer of the cladding acts as the high reflectivity mirror of the 2D GTI structure. In our present simulation, we choose three different silica (high index) layer thicknesses for partial reflector layers around the core, which are 10, 20 and 30% of the thickness of the high index layers forming the QW stack Bragg mirror design. The results of the FE computations clearly show that a reversed dispersion slope can be achieved in a relatively wide wavelength range (see Fig. 4). In our models, the L_0 spacing between the cladding and the thin partial reflector layer had to be set at 0.39, 0.235 and 0.159 times the spacing between the fused silica layers in the QW stack design, respectively. The reversed dispersion slope regimes corresponding to the different partial reflector layers are 260, 220 and 180 nm, respectively. Though the dispersion curve corresponding to the $d_0 = 0.1d$ GTI layer is slightly blue shifted relative to the corresponding dispersion curve obtained for the 1D model calculations, this effect

#96268 - $15.00 USD Received 20 May 2008; revised 24 Jul 2008; accepted 12 Sep 2008; published 18 Sep 2008

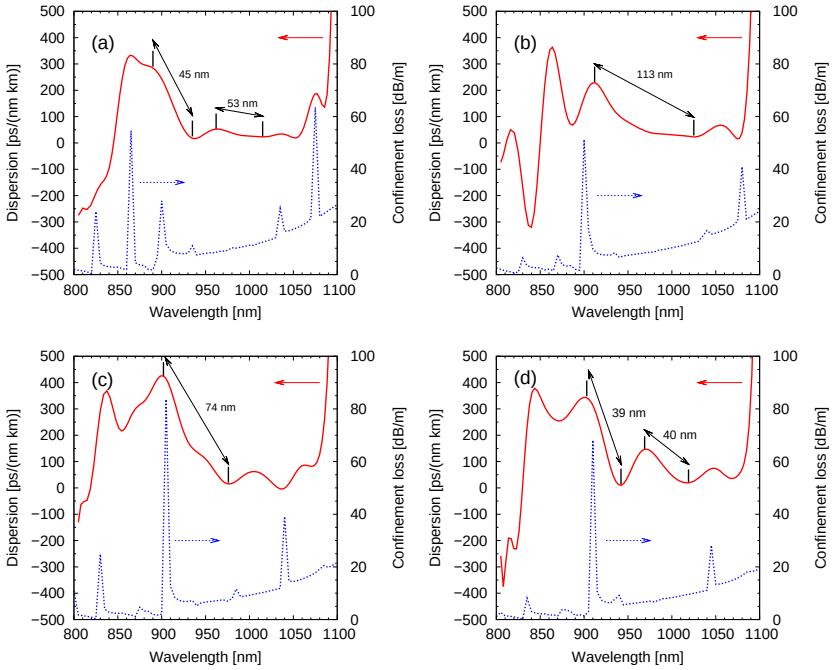

Fig. 5. Dispersion and loss profiles of all-silica HC Bragg fibers with 40 nm thick silica struts. $d = 0.25\ \mu$m, L = (a) 1.24, (b) 1.27, (c) 1.30 and (d) 1.33 μm. The GTI layer had the physical thickness of $d_0 = 0.1d$ and the air spacer thickness was set to $L_0 = 0.75L$.

can be easily canceled by readjusting the spacing between the partial reflector layer and high reflectivity stack.

In order to have an insight into physical effect of the cylindrical GTI layer, what we can regard as a misaligned first period as well, we computed the mode field distributions at different wavelengths, the result of which simulation is shown in Fig. 4(b). The superimposed GTI layer contribute to the effective index of the LP_{02} mode in resonant way through the frequency dependent mode field distribution: clearly, the ratio between the peak and side-lobes gradually varies around the resonance wavelength which leads to the desired reversed dispersion slope.

For the computation of the dispersive functions of complete HC all silica Bragg fiber geometries, we included the previously disregarded silica struts between the fused silica layers in our FE simulations. According to 1D simulations, the wavelength range over which the dispersion slope is reversed is 135 nm wide (987-1122 nm), when the refractive index of the low index spacer layer has the value of 1.02 due to the index raising effect of silica struts. Based on this estimation, we choose the following design parameters for our FE computations: $d = 0.25\ \mu$m, $L = 1.24\ \mu$m, $d_0 = 0.1d$, $L_0 = 0.75L$ and the thickness of silica struts is set to $t_s = 40$ nm.

The corresponding dispersion and loss functions are shown in Fig. 5. It can be seen that leaking-modes appearing within the bandgap reduce the usable bandwidth of the reversed dispersion slope Bragg fiber and they affect the shape of the dispersion function as well. The dispersion function is split to negative and positive slope regimes due to the mode anti-crossing events (or surface modes) and leaking modes. The computed loss function shows that the attenuation of the investigated mode is increased significantly at around the wavelengths where the dispersion function has an inflexion point. For this initial structure, reversed slope regimes of 45 and 53 nm bandwidths could be achieved. We note, however, that the 45 nm wide reversed

#96268 - $15.00 USD Received 20 May 2008; revised 24 Jul 2008; accepted 12 Sep 2008; published 18 Sep 2008

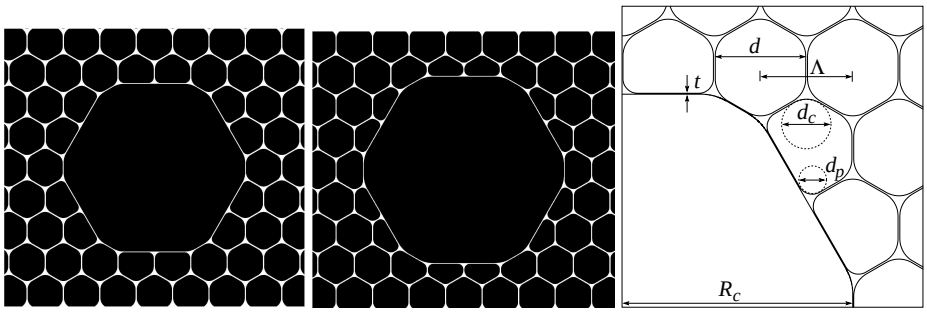

Fig. 6. (a) the modeled 19-cell HC PBG fiber with hexagonal lattice, (b) HC PBG fiber with expanded core (reduced first, low index layer), (c) design parameters of the honey-comb cladding.

dispersion slope regime originates from two physical effects, partially from the effect of the GTI layer, and partially from the effect of the leaking mode appearing at around 900 nm. In order to broaden the usable bandwidth of the reversed dispersion slope regime, we modified the thicknesses of the low index air spacer layers of the Bragg reflector in the following designs. Fig. 5 (b), (c) and (d) show the loss and dispersion profiles of HC Bragg fibers with air spacer layers with thicknesses of L= 1.27, 1.3 and 1.33 μm, respectively. Thickness of the air spacer layer of the GTI design was also rescaled to $L_0 = 0.75L$ in all of these cases. Having a look at Fig. 5, we can observe that the dispersion and loss functions as well as the appearance of leaking modes strongly depend on small structural modifications: a few percent modification in the thickness of the low index air spacer layers may result in dramatic changes in the dispersive properties of the HC Bragg fiber. This behavior is similar to that of chirped mirrors, i.e. 1D chirped dielectric Bragg mirrors [20] widely used for dispersion control in femtosecond pulse solid state lasers. Though the overall dispersion functions show the desired reversed tendency of the dispersion slope, the resonances originating from the leaking modes break up the monotonic nature of these functions. In some specific cases (see Fig. 5 (b)), we obtained a reversed slope over more than 100 nm bandwidth, however, the fourth- and higher-order dispersion contributions may be harmful in such dispersive HC fibers. Further investigations aiming for the reduction of leakage loss and higher-order dispersion terms in PBG fibers with zero or negative dispersion are necessary for introducing these novel dispersive fiber optic devices in practice.

3.3. All air-silica HC fiber of honey-comb structure

Honey-comb structured HC PBG fibers are widely used for dispersion compensation in femtosecond pulse laser oscillators, for pulse compression in femtosecond pulse fiber amplifiers and for nonlinear distortion free delivery of high intensity pulses, due to their low loss and good reproducibility. In these fibers, the above mentioned problems relating to leaking modes appearing within the bandgap are basically solved [11, 29, 31]. In the following, we present our computational results for HC PBG fiber designs of 2D GTI structure, in which a honey-comb structured cladding provides low loss and leaking mode free operation over the reversed dispersion slope regime. This attractive feature makes these novel designs well suited for high quality broadband dispersion control in femtosecond pulse fiber lasers and amplifiers.

In order to obtain a high bandwidth PBG, we have to apply a very high air-filling fraction in the design, which leads to the fact that the air-holes in the cladding tend to be hexagonal in

#96268 - $15.00 USD Received 20 May 2008; revised 24 Jul 2008; accepted 12 Sep 2008; published 18 Sep 2008

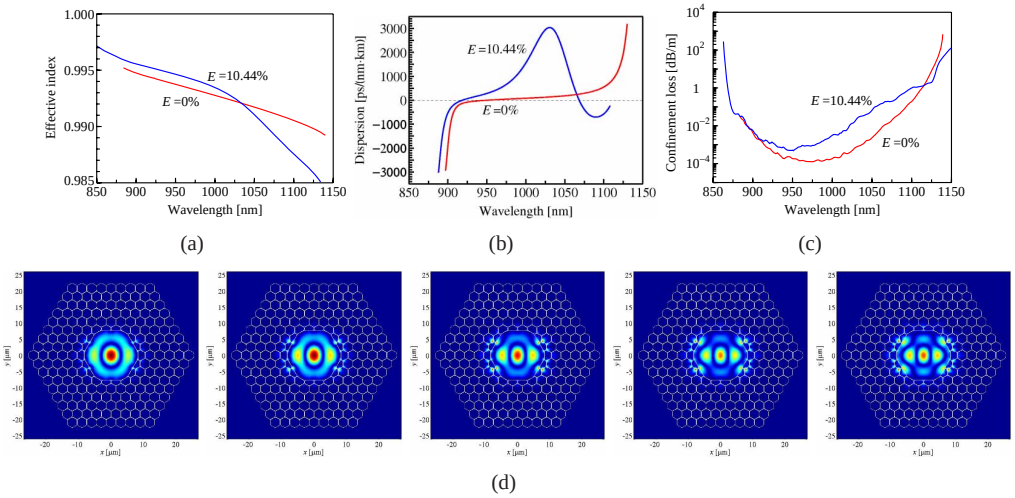

Fig. 7. (a) effective indices obtained with 0 and 10.44% core expansion coefficients for LP_{02} mode, (b) dispersion where reversed slope is obtained over 55 nm, (c) confinement loss and (d) mode field distributions at 1000, 1025, 1050, 1075 and 1100 nm (from left to right).

shape with rounded corners, as shown in Fig. 6. In Fig. 6(a), we model a realistic standard 19-unit-cell hollow-core PBG fiber without core expand, where the cladding holes are represented by hexagons with rounded corners described by the relative hole diameter, d/Λ, and the relative diameter of curvature at the corners, d_c/Λ, with Λ being the hole pitch. The corners of the pentagons surrounding the hollow-core are rounded using circles of relative diameter d_p/Λ. The hexagonal core with rounded corners is defined by a thin silica ring of nearly constant thickness t at the boundary of the cladding. We consider the 19-unit-cell hollow-core PBG fiber, since the higher-order LP_{02} mode is well confined without high confinement loss. It is known that the coupling between the air-guiding mode and the surface mode is a major source of propagation loss in hollow-core PBG fiber and this coupling results in a reduction of the transmission bandwidth making the presence of surface modes the limitation to the development of hollow-core PBG fiber with low attenuation and a broadband transmission spectrum. However, if we appropriately determine the thin silica ring thickness t, we can suppress the presence of surface mode from PBG range [29]. In the following calculations, the silica ring thickness is fixed as $t = 0.5(\Lambda - d)$ for broadband suppression of surface mode [31].

In order to modify the distance of the partial reflector layer from the rest of the structure, we increased the core radius without affecting rest of the structure shown in Fig. 6(b). The core size is determined by parameter R_c as shown in Fig. 6(c), and it is expressed as

$$R_c = (E+1)(2.5\Lambda - t/2) \tag{6}$$

where E stands for an expansion coefficient.

In Figs. 7(a) and (b), we show the effective index curves and the dispersion curves for the LP_{02} mode, respectively, as a function of wavelength, where $d/\Lambda = 0.98$, $d_c/\Lambda = 0.40$, $d_p/\Lambda = 0.30$, $\Lambda = 3.0\ \mu$m, and the expansion coefficient is set to $E = 0\%$ and 10.44%. As we expect, the reversed dispersion slope is obtained at around the 1064 nm wavelength by expanding the core size and decreasing the thickness of the first low index layer. The expansion coefficient of 10.44% corresponds to the core size increment of 0.26Λ from the original core size shown in Fig. 6(a). The wavelength range where the reversed dispersion slope is achieved is about 57 nm

#96268 - $15.00 USD Received 20 May 2008; revised 24 Jul 2008; accepted 12 Sep 2008; published 18 Sep 2008

without changing the thickness of the core wall. Due to the high air-filling fraction and the small silica ring thickness t, the GTI can be constructed by reducing the size of the first low index layer. In order to achieve a wider range of reversed dispersion slope, the air filling fraction must be decreased to be able to adjust t as well. The increase of silica thicknesses, however, leads to the leaking mode problem, which has been discussed in details in the previous section (Sec. 3.2) entitled HC Bragg fiber. Figure 7(c) shows the wavelength dependence of the confinement loss for the LP_{02} mode in hollow-core PBG fiber with 6-ring structure. The confinement loss is less than 0.2 dB/m at 1064 nm.

Finally, we have some comments on the design of air-silica HC fibers of honey-comb structure. In our present calculations, the value of d/Λ had a fixed value of 0.98 in order to obtain broad bandgap at around 1 micron. Of course, one can use lower values of 0.97 or 0.96 at the expense of reduced bandgap. The negative dispersion slope (S) and the corresponding bandwidth can be controlled by changing parameters d_c/Λ, t and E. By increasing the value of d_c/Λ, the negative dispersion slope can be decreased and the bandwidth can be widened. In this case, the negative dispersion slope range is shifted to longer wavelength range. By optimizing the thickness t, the bandwidth can be maximized. The presented results correspond to $t = 0.5(\Lambda - d)$ to suppress the surface mode, and it was not an "optimized" value. By increasing the expansion coefficient E, the negative dispersion slope range can be shifted to shorter wavelength range. The results in Fig. 7 were computed for a higher-order mode, however, like in case of the SC Bragg fiber, our recent simulations show that we can achieve negative dispersion slope even also for the fundamental mode, which might be advantageous in practice.

4. Conclusions

We reported on 1D and 2D simulation results on the dispersive properties of different SC and HC Bragg PBG fiber designs. We have shown that the dispersion slopes of SC and HC Bragg PBG fibers and also a realistic all-silica HC PBG fiber with honey-comb structured cladding can be changed by the addition of a partial reflector layer at the top of the core, which design can be regarded as a 2D equivalent of the well known 1D, single-cavity GTI type dispersive dielectric mirror. Based on the obtained electric field distributions of the preferred higher-order mode as a function of wavelength, we can say that the reversed dispersion slope originates from the GTI effect in these novel PBG fiber designs. At around the resonance wavelength, a higher energy is stored in the cylindrical GTI layer leading to a considerable cubic phase contribution. The presented designs can be easily adapted to other wavelengths by rescaling the geometry followed by some refinement process. We are convinced that these novel fiber optic devices will be well suited for broadband dispersion control in femtosecond pulse fiber lasers, amplifiers and fiber optical parametric oscillators.

Acknowledgment

The financial support of the Hungarian Scientific Research Fund (OTKA, grants T49296 and K76404) is gratefully acknowledged.

#96268 - $15.00 USD Received 20 May 2008; revised 24 Jul 2008; accepted 12 Sep 2008; published 18 Sep 2008